Spora: A Journal of Biomathematics

Volume 2 | Issue 1 Article 5

2016

Sperm Pairing and Measures of Efficiency in Planar Swimming Models

Paul Cripe
Tulane University, pcripe@tulane.edu

Owen Richfield
Tulane University, orichfie@tulane.edu

Julie Simons
The California Maritime Academy, jsimons@csum.edu

Sperm Pairing and Measures of Efficiency in Planar Swimming Models

Cover Page Footnote
The work of PC, OR, and JS was supported, in part, by the National Science Foundation grant DMS-104626. The authors would like to thank the Center for Computational Science at Tulane University for their support, in particular Professor Ricardo Cortez and Professor Lisa Fauci for helpful discussions.

Intercollegiate Biomathematics Alliance

SPORA
A Journal of Biomathematics

ISSN 2473-3067 (Print)
ISSN 2473-5493 (Online)

Sperm pairing and measures of efficiency in planar swimming models

Paul Cripe[1], Owen Richfield[1], Julie Simons[2,*]

*Correspondence:
Prof. Julie Simons, Dept. of Sciences and Mathematics, California Maritime Academy, 200 Maritime Academy Dr., Vallejo, CA 95490-8181 USA
jsimons@csum.edu

Abstract

Sperm of certain species engage in cooperative swimming behaviors, which result in differences in velocity and efficiency of swimming as well as ability to effectively fertilize the egg. In particular, *Monodelphis domestica* is a species of opossum whose sperm often swim cooperatively as a pair, with heads fused together. In order to understand the empirical effects of cooperative swimming behaviors, we propose a simple preferred-curvature-based model to model individual and paired sperm using the method of regularized Stokeslets to model the viscous fluid environment. The effects of swimming freely versus paired swimming, phase relationship, and the angle at which sperm heads are fused are investigated. Results are consistent with previous modeling work for free swimmers. Paired (fused) swimming results also compare well with experimental work and provide evidence for optimal geometrical configurations. This indicates that there may be a fluid mechanical advantage to such cooperative motility behaviors in sperm swimming.

Keywords: Sperm motility, cooperativity, planar waveforms, regularized Stokeslets

1 Introduction

Sperm motility is a complex behavior that varies significantly across species and is arguably the most important indicator for fertilization potential. Widely believed to be subject to strong evolutionary pressures, gamete evolution has been the subject of many studies, particularly in the context of sperm competition and mating strategies (see [1, 15, 24, 25]). On the other hand, sperm cooperativity and collective swimming behavior have received far less attention from a mathematical modeling standpoint, despite substantial experimental evidence in several species [7, 11, 12, 14, 17, 19, 18]. In this context, cooperativity refers to swimming in a coordinated fashion in pairs or groups, or otherwise helping fellow sperm to successfully reach and fertilize the egg.

From an evolutionary standpoint, variations in behavior and morphology across species may correspond to advantages in survival. Reproductive biology is a natural testing ground for these types of investigations, where the assumption is that successful reproduction is the ultimate goal for the survival of the species. In sexual reproduction, successful fertilization of the oocyte is necessary for a specie's survival. In general, sperm motility has a strong positive correlation with successful fertilization of the oocyte [26, 2]. Cooperative motility, therefore, would also have an impact upon fertility potential.

Species as diverse as bulls, insects, opossums, mice, and echidnas have all shown evidence of cooperative sperm motility behavior. It has been shown that two freely swimming bull sperm will synchronize their beats and align to swim with higher velocities as a pair [36]. In the fishfly, sperm form what are called bundles, which may enable the group of sperm to move more efficiently towards the egg [9]. Some rodents even have apical hooks on their sperm heads allowing them to connect to flagella of other sperm [11]. In the case of some deer mouse species, sperm cells swim close together and agglutinate in large groups, sometimes referred to as "sperm trains," leading to increased swimming velocities [7]. The subject of this work is to investigate the sperm of the grey short-tailed opossum, *Monodelphis domestica*, whose sperm "pair" or fuse at the head to create dual-flagella swimmers that swim approximately 23.8% faster than a single sperm swimming alone [17, 19].

While cooperative behavior appears to increase swimming velocities in some species, this may come with a tradeoff. For instance, linking together can cause a significant portion of the sperm population to undergo a premature acrosome reaction or become immotile upon separation [17, 27]. Both of these results would render the sperm infertile. Therefore, these cooperative behaviors may not benefit all individuals, but rather a subset of the group from the perspective of fertilization potential. A primary focus of this paper is to provide quantitative

[1]Mathematics Department and the Center for Computational Science, Tulane University, New Orleans, LA, [2]Department of Sciences Mathematics, California Maritime Academy, Vallejo, CA

results of the effects cooperative behaviors have on velocity and efficiency.

More specifically, we will investigate the efficiency of various paired swimming behaviors using a mathematical model for flagellar motility in low Reynolds number, viscous fluid. We base our model on the preferred curvature flagellum model developed in [6] and the method of regularized Stokeslets [3, 4].

While many models have been proposed for sperm motility, there has been less attention paid to the interaction of two or more sperm. The first investigations into the behavior of oscillatory sheets and filaments in viscous fluids was that of G. I. Taylor [32, 33]. In [32], it was shown that in-phase oscillations minimize the work done by two parallel sheets. These results suggest that there might be an energetic explanation for experimental observations that sperm tend to swim in phase. More recently, [16] have shown that energy dissipation is minimized when infinite cylindrical filaments oscillate in phase in a three-dimensional fluid in various geometrical configurations.

Finite length filaments representing sperm flagella have been investigated in several contexts more recently. In a two-dimensional fluid, oscillating filaments were shown to synchronize and attract in [37]. Energy consumption was also minimized when phase differences between two filaments were small. The work of [13] analyzed the cooperative behavior of semiflexible swimmers for various initial configurations to understand the effect of the distance between two swimmers upon their velocity and efficiency. The recent model of [28] and work in [22] also provide intuition for the long-range interactions of two freely swimming sperm. None of these models, however, address the impact of fusing at the head (or otherwise bonding) upon sperm motility.

In the following sections, we briefly introduce the relevant equations of motion used to capture viscous, Newtonian fluids. Then we derive the flagellum model used to capture the general behavior of sperm motility and further develop this model by incorporating the ability for two flagella to "fuse" at the head. Such fused pairs are designed to reproduce the behavior observed in *M. domestica* sperm pairing. Additionally, freely swimming sperm pairs in close proximity will be analyzed under varying cases, the results of which will be compared to the results of [13]. We then use these results to understand the potential advantages of cooperative swimming behaviors among sperm, and discuss the biomechanical evolutionary pressures that might influence sperm motility and morphology.

2 Methods

2.1 Fluid model

Due to their microscopic size and velocity scales, sperm move in a viscous fluid with a Reynolds number on the order of 10^{-4} to 10^{-2} (see Table 1). Therefore, inertial effects are assumed to be negligible. As such, the incompressible Stokes equations are used to model the governing fluid dynamics:

$$\begin{aligned} \mu\Delta\mathbf{u} &= \nabla p - \mathbf{F}(\mathbf{x}) \\ \nabla\cdot\mathbf{u} &= 0 \end{aligned} \tag{1}$$

where $\mathbf{u}$ is the fluid velocity, μ is the dynamic viscosity, p is pressure, and $\mathbf{F}$ is the external force density (force per unit volume).

The flagellum is modeled as a curve $\mathbf{X}(s,t)$, denoting the spatial position of the flagellum at arc length s and time t. As the flagellum moves, this curve will exert forces along its length, resulting in the following definition of the force density $\mathbf{F}(\mathbf{x})$:

$$\mathbf{F}(\mathbf{x}) = \int_0^L \mathbf{f}\big(\mathbf{X}(s,t),t\big)\phi_\epsilon\big(\|\mathbf{x}-\mathbf{X}(s,t)\|\big)\,ds \tag{2}$$

where $\mathbf{f}\big(\mathbf{X}(s,t),t\big)$ describes the local force the flagellum is exerting at arc length s and time t. In this expression, L is the length of the flagellum, and ϕ_ϵ is a regularized delta function that distributes the forces $\mathbf{f}$ in a small fluid around the curve $\mathbf{X}(s,t)$. Following the methodology used in [4], we let

$$\phi_\epsilon(r) = \frac{15\epsilon^4}{8\pi\big(r^2+\epsilon^2\big)^{7/2}}. \tag{3}$$

The parameter ϵ should be thought of as a small parameter chosen to be roughly of the same order as the radius of the flagellum.

A Stokeslet is a fundamental solution to the incompressible Stokes equations (1) given a singular point force. Because we are considering forces that are effectively "spread out" in a fluid volume around the curve $\mathbf{X}(s,t)$, we will instead use a regularized Stokeslet solution to the incompressible Stokes equations (1). As described in [4], the regularized Stokeslet for the regularized delta function (3) given a force $\mathbf{f}$ at a position $\mathbf{x}_0$ is

$$\mathbf{u}(\mathbf{x},t) = \frac{\mathbf{f}\big(r^2+2\epsilon^2\big) + \big(\mathbf{f}\cdot(\mathbf{x}-\mathbf{x}_0)(\mathbf{x}-\mathbf{x}_0)\big)}{8\pi\mu\big(r^2+\epsilon^2\big)^{3/2}}$$

where $r = \|\mathbf{x}-\mathbf{x}_0\|$. Because the equations (1) are linear, if we have more than one point force in the fluid, we simply add the regularized Stokeslets together to find the total velocity field.

Table 1: Typical scales representative of mammalian sperm.

Quantity	Description	Value	References
L	Length (sperm length)	100 µm	[5]
T	Time (from beat frequency)	0.1 s	[21]
V	Velocity: wave speed, L/T	10^{-3} m/s	[31]
μ	Viscosity (water)	10^{-3} kg m^{-1}s^{-1}	
p	Pressure $\left(\frac{\mu U}{L}\right)$	10^{-2} Pa	
F	Force density $\left(\frac{\mu U}{L^2}\right)$	10^{2} N/m^3	
Re	Reynolds number	10^{-2} to 10^{-4}	

2.2 Flagellum Model

Many mathematical investigations into sperm motility have considered the swimming of individuals with planar waveforms, because sperm flagella exhibit nearly planar, sinusoidal waveforms [10, 30, 35]. For simplicity and to facilitate comparison with previous models, we will assume a planar motion as well. Additionally, we will assume that paired sperm have flagella beating in the same plane, to best model the behavior observed in opossum sperm such as *M. domestica*. Thus, we will only consider the effects of planar cooperative swimming. Each flagellum will be modeled following the planar preferred curvature model first derived in [6] and subsequently used to model sperm motility with biologically-relevant swimming velocities and beat amplitudes in [23].

As in [6], the flagellum model relies upon an energy formulation that can be expressed as

$$\mathcal{E}(\mathbf{X},t) = \mathcal{E}_{tens}(\mathbf{X},t) + \mathcal{E}_{bend}(\mathbf{X},t)$$

where

$$\mathcal{E}_{tens}(\mathbf{X},t) = \tfrac{1}{2}S_t \int_0^L \left[\left\| \frac{\partial \mathbf{X}}{\partial s} \right\| - 1 \right]^2 ds$$

$$\mathcal{E}_{bend}(\mathbf{X},t) = \tfrac{1}{2}S_b \int_0^L \left[\left(\frac{\partial \mathbf{X}}{\partial s} \times \frac{\partial^2 \mathbf{X}}{\partial s^2} \right) \cdot \hat{\mathbf{z}} - C(s,t) \right]^2 ds.$$

In this formulation, the flagellar beat plane is the xy-plane and $\hat{\mathbf{z}}$ is the unit vector in the z-direction (out of the beat plane). The energy $\mathcal{E}_{tens}$ models the tensile energy, which keeps the flagellum approximately inextensible. The energy $\mathcal{E}_{bend}$ is the bending energy that causes the flagellum to bend *locally* towards a preferred curvature given by $C(s,t)$, which is taken to be a time-dependent sinusoidal waveform:

$$C(s,t) = k^2 b \sin(ks - \omega t + \phi_0). \tag{4}$$

This curvature has wavenumber k, frequency ω, and may be shifted by a phase given by ϕ_0. The parameter b is an amplitude scaling factor.

Forces are derived from these energies by letting

$$\mathbf{f}(\mathbf{X},t) = -\frac{d\mathcal{E}(\mathbf{X},t)}{d\mathbf{X}}.$$

Such an energy formulation ensures that the flagellum is seeking out a minimal energy configuration that evolves over time due to the preferred curvature waveform. For further details on the derivation of this model, see [6].

2.3 Discretized Model

For computational purposes, we will discretize the curve $\mathbf{X}(s,t)$ and the forces $\mathbf{f}$ as follows:

$$\mathbf{X}_j(t) = \mathbf{X}(j\Delta s, t)$$
$$\mathbf{f}_j(t) = \mathbf{f}(\mathbf{X}_j, t)$$

where there are N points along the flagellum, separated by a preferred arc length distance of Δs, and $j = 1, \ldots, N$ denotes the point along the flagellum. Thus, $N\Delta s = L$, the total length of the flagellum.

The discretized forces $\mathbf{f}_j$ are derived from a discretized approximation of the energy formulations given in Section 2.2. The discretized total energy, denoted by $E = E_{tens} + E_{bend}$, is found using the following discrete forms:

$$E_{tens} = \tfrac{1}{2}S_t \sum_{j=2}^{N} \left(\left\| \frac{\mathbf{X}_j - \mathbf{X}_{j-1}}{\Delta s} \right\| - 1 \right)^2 \Delta s$$

$$E_{bend} = \tfrac{1}{2}S_b \sum_{j=2}^{N-1} \left(\frac{(x_{j+1} - x_j)(y_j - y_{j-1})}{\Delta s^3} - \frac{(y_{j+1} - y_j)(x_j - x_{j-1})}{\Delta s^3} - C_k(t) \right)^2 \Delta s$$

where $\mathbf{X}_j = (x_j, y_j)$. Then, we calculate the forces $\mathbf{f}_j$ located at positions $\mathbf{X}_j$ given by solving $\mathbf{f}_j = -\frac{dE}{d\mathbf{X}_j}$. Figure 1 depicts the components of this discretized flagellum model.

As in [4], the velocity field $\mathbf{u}(\mathbf{x},t)$ is found from the forces $\mathbf{f}_j$ by exploiting the linearity of the equations (1). Thus, $\mathbf{u}(\mathbf{x},t)$ can be expressed as a summation of regularized Stokeslets:

$$\mathbf{u}(\mathbf{x},t) = \sum_{j=1}^{N} \frac{\mathbf{f}_j\left(r_j^2 + 2\epsilon^2\right) + \left(\mathbf{f}_j \cdot (\mathbf{x} - \mathbf{X}_j)(\mathbf{x} - \mathbf{X}_j)\right)}{8\pi\mu\left(r_j^2 + \epsilon^2\right)^{3/2}}.$$

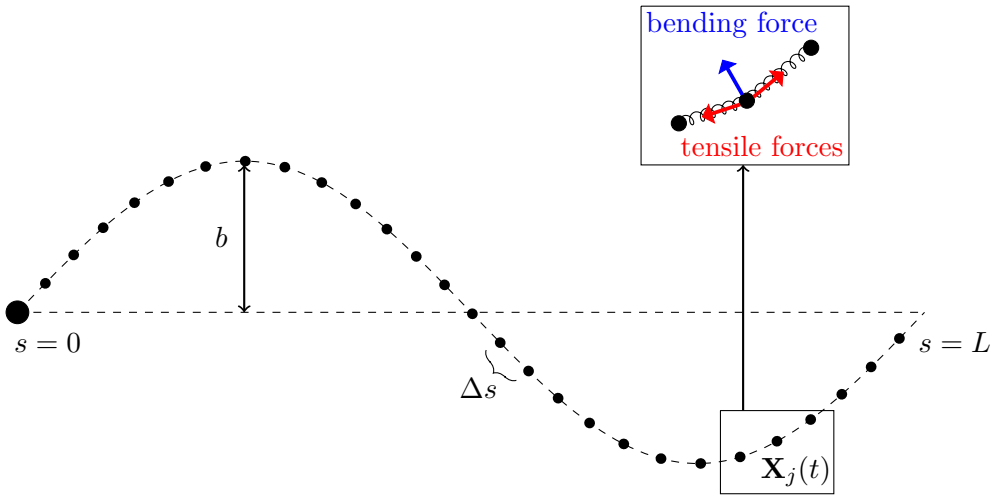

Figure 1: A diagram of the idealized flagellum configuration with total arc length L and amplitude b. The flagellum is discretized, denoted by points $\mathbf{X}_j(t)$ where j is the index of the point. Tensile forces keep the flagellum approximately inextensible while preferred curvature (bending) forces cause the sinusoidal motion of the flagellum. The head of the sperm is depicted by a large point at arc length $s = 0$.

We define the radial distances as $r_j = \|\mathbf{x} - \mathbf{X}_j\|$.

2.4 Models for Paired Swimmers

Sperm cooperation and motility are explored in several different contexts by considering cases of sperm swimming in close proximity (but disconnected or freely swimming) as in [13] and fused-head swimmers reminiscent of *M. domestica* sperm. Both styles of swimmers (free-swimming/disconnected versus fused), will be compared to a single sperm swimming alone using velocities, power and efficiency (see Section 3).

In the case of disconnected sperm swimming in close proximity, the starting distance between the flagella, d_0, will be varied along with the phase relationship of the two swimmers, as shown in Figures 3a and 3b. For the fused-head model, we will investigate the effects of phase as well as the angle at which the flagella are connected.

To model a fused-sperm pair, we connect the first several points on each flagella to each other using tensile (spring) forces similar to those used to keep the flagellum points together. To prevent sliding effects and maintain the desired head geometry, we use forces that cross-connect the points as well. These tensile forces serve to effectively fuse the two heads together. Figure 3c shows an example of a fused-head configuration where the two flagella are out of phase with respect to each other, with heads at an angle of θ with respect to each other. This angle determines the resting length of the tensile (spring) forces that connect the first several points. For more details on the geometry of the fused-head model, see A).

We note that we do not have a true head for the sperm in our model; this is done so that we can compare our model to the work in [13]. However, the fused pairs are connected using the first six points along each flagellum (chosen to mimic the typical length of a mammalian sperm head compared to the flagellum length, see [5] for typical dimensions). Because these points are chosen to represent the "heads" of the sperm pair, they will not experience curvature forces, unlike the rest of the points along the flagella.

2.5 Repulsion Forces

In order to address the physically unrealistic scenario of two flagella crossing within their planar configuration, we use a repulsive force to prevent this from happening, as used in [28]. This repulsion is a force that is only non-zero if two points on separate flagella come within a fixed repulsion distance d of each other. The repulsion force will take the following form, for two points $\mathbf{X}_j$ and $\mathbf{X}_k$ which are on separate flagella:

$$\mathbf{g}_{j,k}(t_i) = S_r(\mathbf{X}_k - \mathbf{X}_j)\left(\frac{1}{\min\left(\|\mathbf{X}_k - \mathbf{X}_j\|, d\right)} - \frac{1}{d}\right)$$

where S_r is a strength parameter for the repulsive force. The value of d is set to be larger than both the regularization parameter ϵ and the discretization length scale Δs. Note that as the distance between the points approaches zero, $\mathbf{g}^k_{j,k}$ approaches infinity, which effectively keeps the flagella apart. This repulsion force will be added to the force at point $\mathbf{X}_j$. An equal and opposite force will be added to the force at point $\mathbf{X}_k$. While the repulsion force

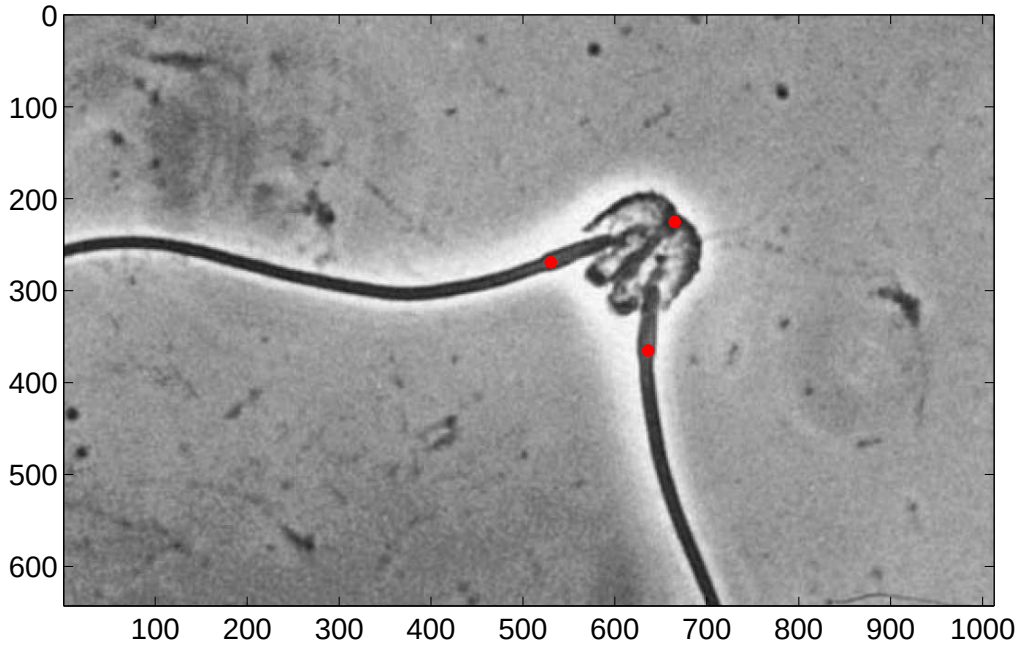

Figure 2: Image of opossum sperm heads attached to each other, reproduced with permission from [19]. Red dots have been super-imposed to demonstrate the way the angle between the flagella from this experimental image would be calculated. In this image, the angle is approximately 60.2 degrees. Using several similar experimental images of *M. domestica* sperm (Figure 1A from [19] and Figure 3A from [27]), the range of angles was 56.9 to 65.3 degrees with an average of 60.6 degrees.

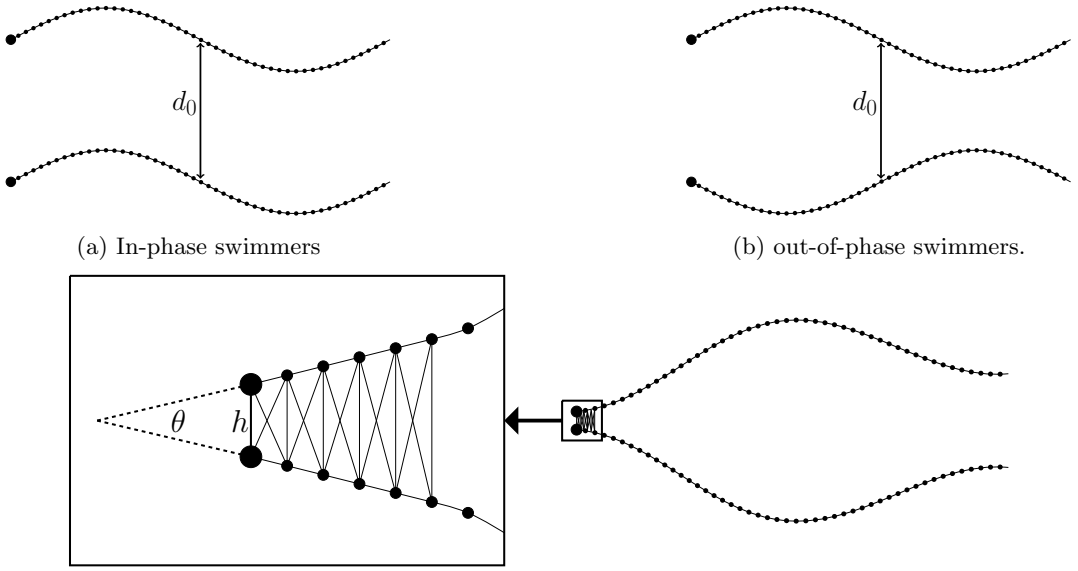

(a) In-phase swimmers

(b) out-of-phase swimmers.

(c) Fused-head pair of swimmers (shown out of phase), with inset (left) showing tensile connections (spring bonds, denoted by solid lines) between flagella points near heads of both flagella.

Figure 3: Depiction of initial configurations of two flagella. In panels (a) and (b), two flagella are initialized a distance of d_0 away from each other for both in-phase and out-of-phase swimmers, respectively. Panel (c) shows the geometry for a fused-head pair (here the pair is depicted out of phase, but the phase relationship between the flagella will be varied). Inset (left) depicts the way the first six points of the flagella are fused to mimic head fusion of paired opossum sperm. The angle θ is changed to investigate the effect of the angle between the flagella on motion. The distance h refers to the distance between the first two points.

Table 2: Parameter values. Wherever possible, values have been chosen to reflect typical mammalian sperm dimensions.

Parameters	Description	Value	Reference
ϵ	Regularization parameter	1.3 µm	
Δs	Spatial (arc length) discretization	1 µm	
L	Flagellum length	100 µm	[5]
b	Amplitude	10 µm	[21]
κ	Wavelength parameter	$2\pi/L$	[28]
ω	Frequency	20π (10 Hz)	[21, 28]
ϕ_0	Phase change parameter	0 to π	
S_r	Repulsion strength	5×10^{-4} aN µm^{-3}	[28]
d	Repulsion radius	2ϵ	
S_t	Tensile stiffness	2 pN µm^{-3}	[29]
S_b	Curvature stiffness	10 pN µm^{-3}	[29]
d_0	Initial distance between disconnected flagella	0.005 µm to 1 µm	
h	Distance between heads of connected flagella	Δs	
θ	Angle between connected flagella heads	17° to 98°	

is not a dominant force in terms of free-swimming behavior of disconnected sperm, it is more important in the fused-head model because we are imposing a constrained geometry at the head and specific phase relationships between the two flagella that may result in unrealistic crossing if the repulsion force were not incorporated.

2.6 Numerical Method

The following steps summarize the numerical method:

1. Initialize our sperm in the configurations depicted in Figure 3.
2. Find forces $\mathbf{f}_j$ for the points $\mathbf{X}_j$ from the total discretized energy E.
3. Calculate repulsive forces $\mathbf{g}_{j,k}$ for all possible k points and add to $\mathbf{f}_j$.
4. Solve for velocities $\mathbf{u}_j$ using the method of regularized Stokeslets [4] with forces $\mathbf{f}_j$.
5. Move all points $\mathbf{X}_j$ using a forward Euler time step with velocities $\mathbf{u}_j$.
6. Repeat steps 2–5.

3 Quantifying Efficiency and Motility

In order to compare different motility patterns, we consider steady state velocity, average power and efficiency. To calculate these quantities, we consider sperm behavior only after a steady state swimming pattern emerges after starting from the initial configurations such as those shown in Figure 3. For instance, the speeds we report (denoted by V) are steady state speeds determined by finding the distance a single point moves after one full beat.

The power exerted by a single-sperm modeled by the curve $\mathbf{X}(s,t)$ swimming with velocities $\mathbf{u}\big(\mathbf{X}(s,t),t\big)$ can be defined as

$$\int_{s=0}^{L} \mathbf{u}\big(\mathbf{X}(s,t),t\big) \cdot \mathbf{f}\big(\mathbf{X}(s,t),t\big) ds. \tag{5}$$

Computationally, we approximate the power exerted by a single sperm by discretizing the above integral and averaging the powers exerted by all flagella in the simulation. Denoting each flagellum with a superscript k for $k = 1, \ldots, M$ where M is the total number of flagella in the simulations, we define the discretized power per flagellum as:

$$P(t) = \frac{1}{M} \sum_{k=1}^{M} \left(\frac{\Delta s}{2} \left(\mathbf{u}_1^k(t) \cdot \mathbf{f}_1^k(t) + \mathbf{u}_N^k(t) \cdot \mathbf{f}_N^k(t) \right) + \sum_{j=2}^{N-1} \mathbf{u}_j^k(t) \cdot \mathbf{f}_j^k(t) \Delta s \right)$$

using the trapezoidal rule to approximate the integral (5) with N total points along the flagellum. We define the average power per beat, $\bar{P}$, as

$$\bar{P} = \frac{\omega}{2\pi} \sum_{n=0}^{N_b} P(n\Delta t)\Delta t. \tag{6}$$

Here, ω is again the beat frequency and N_b refers to the number of time steps in one full beat. In comparing the average power of a paired model to the base case, all

$\bar{P}$-values will be normalized by the average power of a single sperm in isolation, referred to as the base case, denoted $\bar{P}_0$.

The efficiency of a swimming behavior will be quantified using the ratio of the flagellum's average velocity squared to average power, a quantity we refer to as β:

$$\beta = \frac{V^2}{\bar{P}}. \tag{7}$$

This ratio gives a numerical value for efficiency: the higher the β ratio, the higher the velocity for each unit of power exerted, thus the more efficient. The efficiencies of all models will be compared to the efficiency of the base case, denoted β_0. For the purpose of comparison, all β-values will be normalized by β_0.

4 Results

4.1 Free swimmers

We first focus on the interaction between two free (disconnected) swimmers, initialized either in phase or out of phase. We are primarily interested in whether swimmers attract or repel each other and the effects of distance between the swimmers upon velocity and power exerted. As noted in [22, 28], swimmers attract and swim towards each other when they are initialized in phase when they are coplanar, as depicted in Figure 3a. However, when initialized out of phase, we observe that two sperm swim away from each other.

Figure 4 summarizes the results of the free swimming simulations, as functions of velocity, power and efficiency versus distance. These results show both in- and out-of-phase swimmers, as well as two different simulation approaches, which we refer to as "dynamic" and "parallel".

The curves labeled as "dynamic" in Figure 4 refer to the free-swimming-sperm model that is initialized as in Figures 3a and 3b, and then simulated for a long period of time. Over the course of the simulation, the sperm interact with each other via the surrounding fluid. This causes them to swim apart or towards each other, and also results in changes in their relative positional geometry with respect to each other. For instance, as two in-phase sperm swim towards each other, their heads are closer to each other compared to their tails, thus they are no longer in a parallel configuration like the ones depicted in Figure 3a.

We compare these dynamic simulations to simulations where the sperm are placed in parallel configurations (just as in Figure 3a) and swimming is simulated for only a single beat. These simulations are run over a range of separation distances d_0 and labeled "parallel" in the figures. These parallel results are reported in order to remove the effect of the change in relative (positional) geometry between the two sperm over time that we observe in the dynamic case.

Importantly, in the parallel case, the in-phase curve (solid gray curves in Figure 4) is smooth until the separation distance comes within the repulsion radius d. This radius is set to ensure the two flagella do not overlap or occupy the same space concurrently, and the velocity, power, and efficiency curves appear non-smooth because a new force is being added in the simulation only at those close distances.

Conversely, in the dynamic case—when the relative geometry between the two sperm is changing—we observe non-smooth behavior of the curves for the in-phase swimmers (black solid curves in Figure 4) even at larger distances when repulsion is not present. Thus, the jagged behavior of the dynamic case is primarily due to the changing relative geometry as two sperm swim towards each other and impede each others' paths when they are close enough.

We emphasize that the dynamic case is the physically more realistic scenario, as sperm interact with each other in populations over time and this changes their trajectories and orientations with respect to each other. They will never remain in a perfectly parallel configuration over time, regardless of phase or the initial distance of separation.

In general, these results show that velocity, power, and efficiency are lower for in-phase swimmers when compared to a single sperm swimming on its own (represented by the horizontal black line in Figure 4). Velocity does increase somewhat when the in-phase swimmers get within approximately 10–15 µm of each other, but never achieves the velocity of the single sperm.

The converse appears to be true for out-of-phase swimmers, which typically exhibit higher velocities, power, and efficiency than a single sperm. There does appear to be a slight reduction in velocity and efficiency when swimmers are around a distance of 34 µm (or 34% of the flagellum length) away from each other. Near these distances, the increases in power outweigh the velocity gains, resulting in decreased efficiency when compared to a single swimmer. However, as the average distance continues to decrease (swimmers get closer together) the corresponding velocity gains are large enough to dominate the extra forces exerted and increase efficiency.

4.2 Fused-head swimmers

For fused-head swimmers, we initialize the two sperm with their heads connected as shown in Figure 3c. Typical flow fields over the course of a beat for the fused-head model where the two sperm are out of phase are shown in Figure 5. These are cross-sections of a fully three-

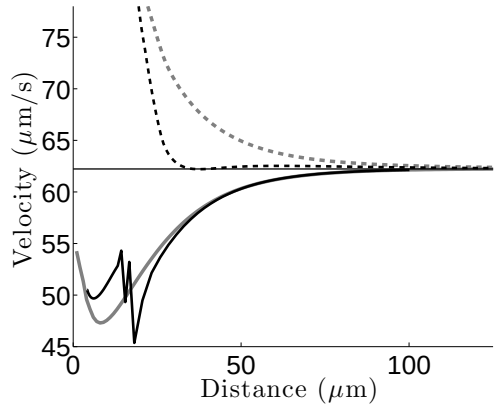

(a) Velocity versus distance.

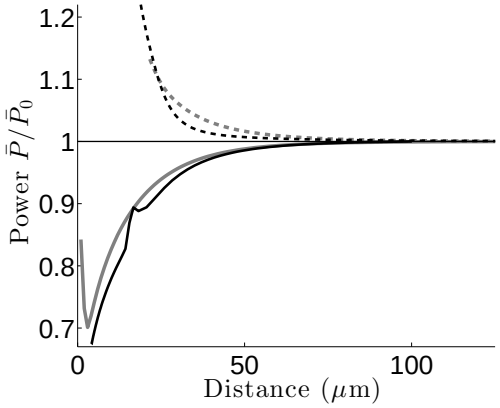

(b) Power versus distance.

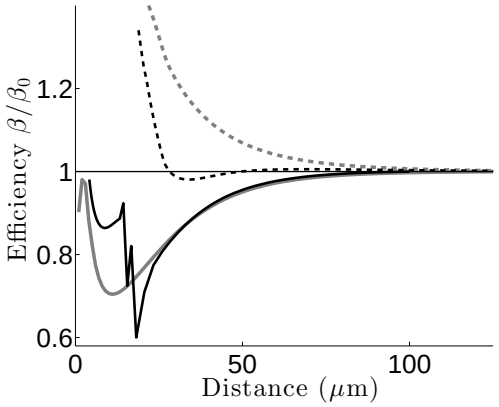

(c) Efficiency versus distance.

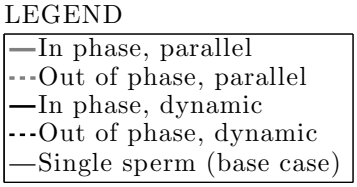

Figure 4: The effect of distance upon velocity, power, and efficiency as two sperm swim freely near each other, either initialized in parallel configurations for a single beat per simulation or as a dynamic simulation where sperm either attract over time (when in phase) or repel over time (when out of phase). Power per beat ($\bar{P}$) and efficiency (β) are normalized by the base case scenario (denoted by $\bar{P}_0$ and β_0) of a single sperm swimming by itself.

dimensional flow. The next two sections investigate the effects of phase and angle upon velocity, power, and efficiency for fused-head swimmers.

4.2.1 Angle of fusion

Figure 6 shows the results of fused-head swimmers with a range of fusion angles θ. It appears that for in-phase swimmers, larger angles serve to decrease velocity and efficiency and increase power. In all the in-phase cases, velocity and efficiency are lower than a single sperm swimming by itself. Power exertion per flagellum per beat ($\bar{P}$) is lower than for a single sperm swimming by itself for smaller angles θ, but larger for angles beyond around 60 degrees.

However, for out-of-phase swimmers, there appears to be an optimal angle that serves to enable the fused pair to swim faster. This comes at a cost in the power exerted per beat ($\bar{P}$): For out-of-phase swimming, the power exerted per flagellum is higher. The efficiency only exceeds the single sperm base case within a particular range of angles (approximately 39 to 67 degrees). The peak is around 61.3 degrees.

Interestingly, this compares well with the angles paired sperm appear to exhibit in experimental images. For instance, Figure 2 shows a typical *M. domestica* sperm pair and three points used to determine the angle of fusion that our model would represent. Using this image as well as Figure 3A from [27], we estimated the range of angles of fusion created by the heads of the sperm to be approximately 60.6 degrees with a standard deviation of 3.1 degrees. The peak in efficiency we find in our model, therefore, is within the range of experimental angles.

4.2.2 Phase changes

Figure 7 shows the effect of varying the phase shift between the preferred curvatures for the two fused sperm. This is done by changing the value of ϕ_0 in the formula given by equation (4): For one flagellum $\phi_0 = 0$, and the other one will have a different ϕ_0, which we will refer to as the phase shift. Both velocity and power increase monotonically as the two sperm tend towards completely out of phase (a phase shift of π). Efficiency exceeds the efficiency of a single sperm swimming by itself for phase shifts between $3\pi/4$ and π. Efficiency is maximized at a phase shift of π, which is the out-of-phase case. Experimental images such as Figure 2 and Figure 3A from [27] also appear to show sperm pairs typically beat in an out-of-phase manner.

5 Discussion

Consistent with biological studies and the work of [13], we have found evidence that sperm engaging in cooperative swimming behaviors can achieve higher velocities and efficiencies than an individual sperm. For detached, freely swimming sperm, our findings compare well with the findings of [13] regarding the relationship between power, velocity and the distance between in-phase and out-of-phase coplanar swimmers. Power and velocity increase for out-of-phase swimmers as distance decreases, and vice versa for in-phase swimmers.

As we have shown in this work, sperm paired at the head can achieve speeds 26.6% faster than an individual. This is the first model to consider this system, but this finding is similar to the biological results in [19], where it is shown that paired *M. domestica* sperm achieve 23.8% higher velocities than single sperm. The distance between the flagella and the angle between the heads can affect the results significantly. It appears that the optimal angle for the fused-head, out-of-phase swimmers is an angle of fusion θ around 61.3 degrees. This result is consistent with the angles depicted in experimental images for opossum sperm of around 60.6 degrees.

This paper also examined the effects of altering the phase relationship between fused-head swimmers. Completely out-of-phase swimmers were the fastest and most efficient configuration. This scenario matches the biological configurations observed in opossum sperm (see [19, 27]). Plotting efficiency and velocity against the phase and angle of connected sperm helps show how the swimming configuration of opossum sperm is optimal in terms of fluid dynamic efficiency and velocity.

6 Conclusion

We have quantified the effects of various cooperative swimming behaviors based upon a planar swimming model previously shown to capture important features typical of mammalian sperm motility. Our results are consistent with other modeling approaches, but also enable comparison with sperm pairing behavior that has not been modeled previously. Remarkably, our results indicate that the sperm pairs observed in *Monodelphis domestica* opossums are in geometrical configurations that seem to optimize efficiency and increase swimming velocities in our model. This also provides a fluid mechanical argument supporting sperm pairing, beyond the observations in [19] that pairs tend to swim in straighter trajectories with higher velocities, which is thought to help the sperm to navigate the oviduct more effectively.

It is clear that morphology and geometry have significant effects upon sperm motility (both for free swimmers

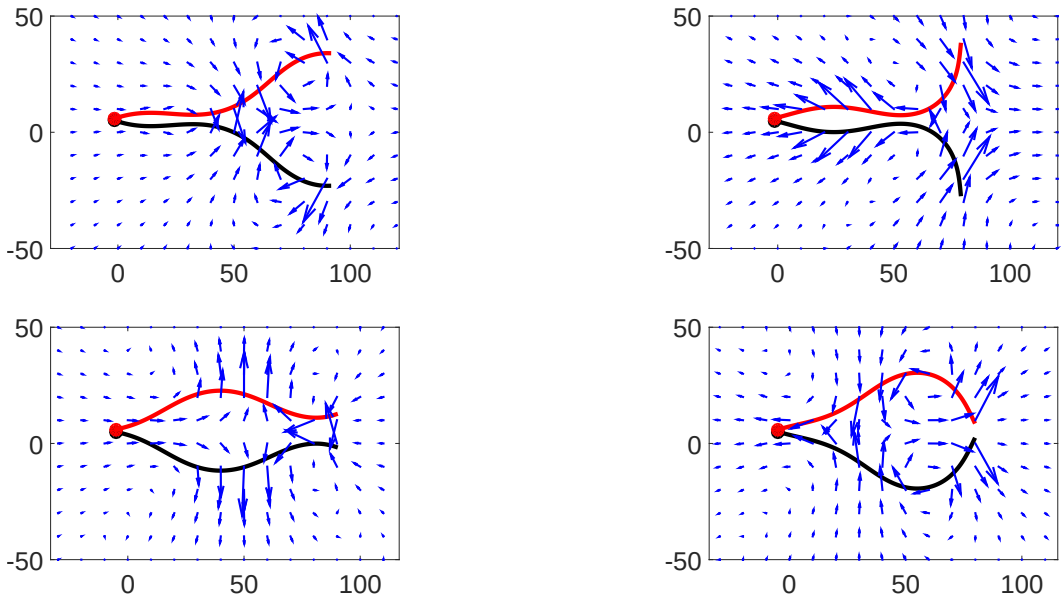

Figure 5: Snapshots of the velocity field over time for two fused sperm with an out-of-phase beat pattern. The images appear chronologically from left to right, top to bottom, with 0.025 seconds (1/4 of a beat) between snapshots. Larger arrows indicate stronger velocities. The two flagella seem to be propelling themselves forward by pushing the fluid behind them. Spatial units are in µm.

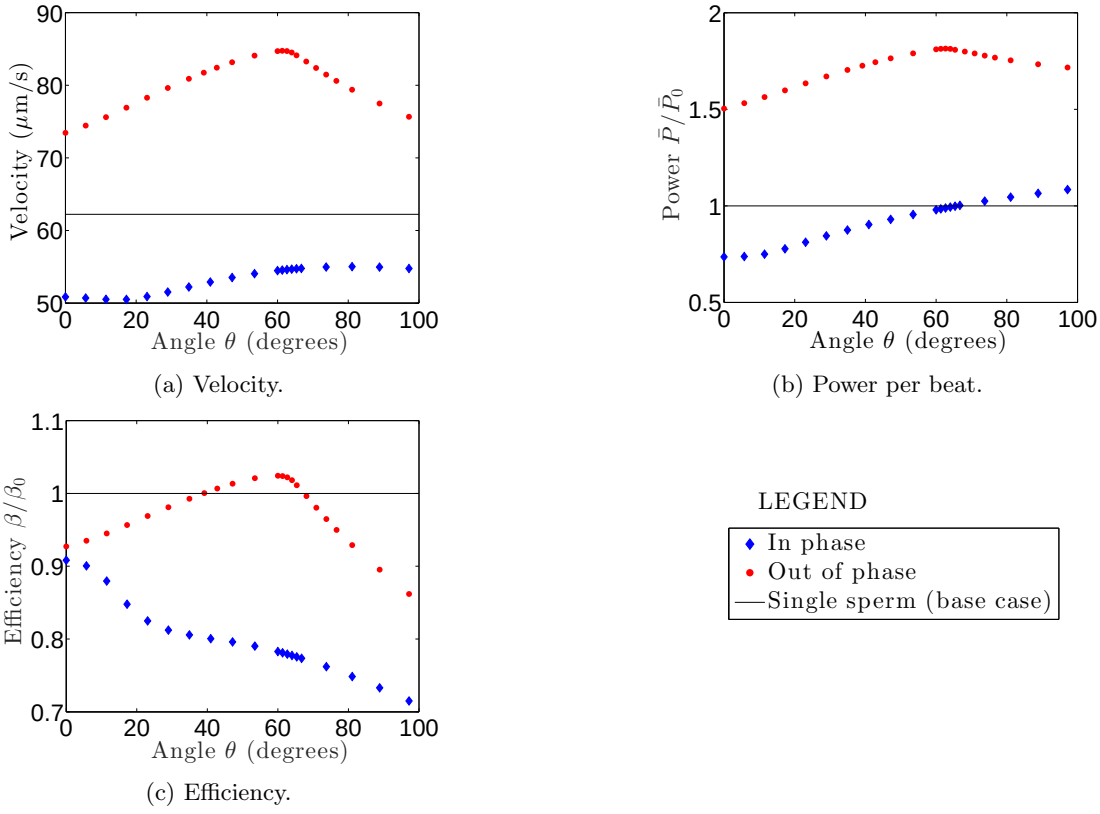

(a) Velocity.

(b) Power per beat.

(c) Efficiency.

Figure 6: The effect of the angle of fusion θ upon velocity, power, and efficiency of two fused-head swimmers. There appears to be an optimal angle (around 61.3 degrees) for all three measures to be maximized for the out-of-phase swimmers (denoted by dots), whereas velocity and efficiency always decrease for the in-phase swimmers (denoted by diamonds). Power per beat decreases for in-phase swimmers, up until an angle of fusion θ of about 60 degrees.

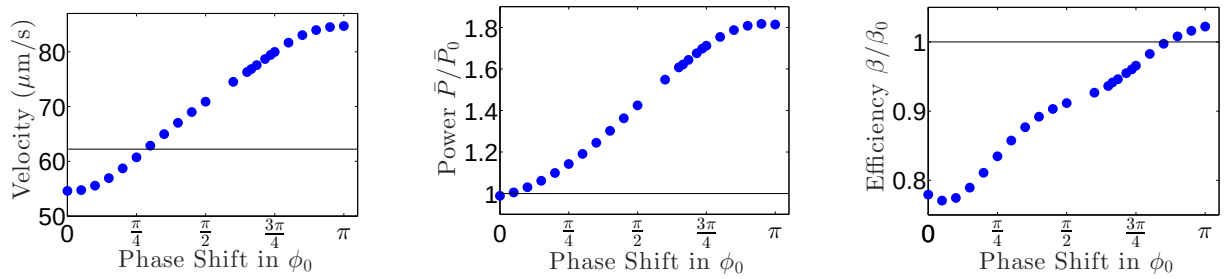

(a) Velocity. (b) Power per beat. (c) Efficiency.

Figure 7: The effect of the phase shift (in ϕ_0) between two fused-head swimmers upon velocity, power, and efficiency (marked by dots). The base case scenario of a single sperm swimming by itself is denoted by the black horizontal lines, for comparison. Both velocity and efficiency increase as the phase shift between the two sperm increases towards π.

and fused-head swimmers). From an evolutionary standpoint, there are many motility criteria (velocity, power expenditure, efficiency, etc.) as well as other fitness criteria that are necessary for fertility on individual and species-wide levels.

For instance, because of the typically harsh environment sperm encounter in the oviduct, there might be evolutionary pressures to favor faster swimming sperm. On the other hand, perhaps the most efficient swimmer might be favored to ensure survival when swimming speeds alone may not capture all of the relevant biological pressures. Factors that influence these preferences include available resources (both from the perspective of the organisms as well as their gametes themselves) and the mating strategies of the species.

One interesting scenario is that of sperm competition in polyandrous species where a female has multiple mating partners. Such species may favor entirely different traits in sperm compared to what might occur in monogamous species [24]. *Monodelphis domestica* opossums are considered a promiscuous species (at least in captivity) where sperm competition might play a role in the evolutionary biology of sperm morphology and behavior [34].

There are several other examples of promiscuous species which also have been shown to exhibit cooperative behavior in sperm, including the deer mouse species *Peromyscus maniculatus* and *Peromyscus polionotus*. Interestingly these two species appear to differ in whether their sperm will cooperate with all other sperm indiscriminately or selectively group with sperm from only the same male [7]. While our model is not meant to capture these behaviors, it does suggest that there may be benefits from such cooperative behavior from a fluid mechanics standpoint.

It has been noted in [11, 17, 20] that cooperativity could arise from a game theoretical perspective, dating back to Hamilton's 1964 paper [8]. The nature of these observations in sperm swimming in groups suggests that a full understanding of the advantage of these different swimming behaviors must include a measure of successful fertilization that includes motility and energy expenditures at the cellular level. Because motility is not only necessary for fertilization, but can lead to a competitive advantage in fertilization in both cooperative and competitive settings, the investigation of group swimming behaviors from a biomechanics perspective may lead to new insights in game theory models.

Besides game theoretic considerations, there are several other factors that should be considered to more fully understand the fluid mechanics of sperm cooperativity. Since our model is currently restricted to solely planar forces, we cannot consider general interactions between sperm or sperm pairs, nor can we consider non-planar flagellar waveforms. While mammalian sperm do exhibit primarily planar waveforms, it is true that the waveforms are not purely planar. We plan on using the recent three-dimensionally robust model proposed in [28] to explore general interactions between sperm individuals and pairs in 3D in order to understand these measures of efficiency and velocities in populations of sperm.

One significant aspect that our model has not investigated, is that in species where sperm pairing occurs, the separation process causes significantly higher occurrences of sperm undergoing a premature acrosome reaction, rendering the sperm infertile [18, 20]. The tradeoff between gains in swimming velocities and number of viable sperm is a question of maximizing utility. Utility, in this context, refers to the probability of successful fertilization, which is correlated with sperm velocity. The primary purpose of this paper is to effectively quantify these velocity and efficiency gains. The data gathered here may in turn be used for further research into the tradeoff and evolutionary pressures of this particular swimming behavior.

Ultimately, any questions regarding sperm cooperativity and competition must consider not just mating strategies or fluid mechanics of individuals, but popula-

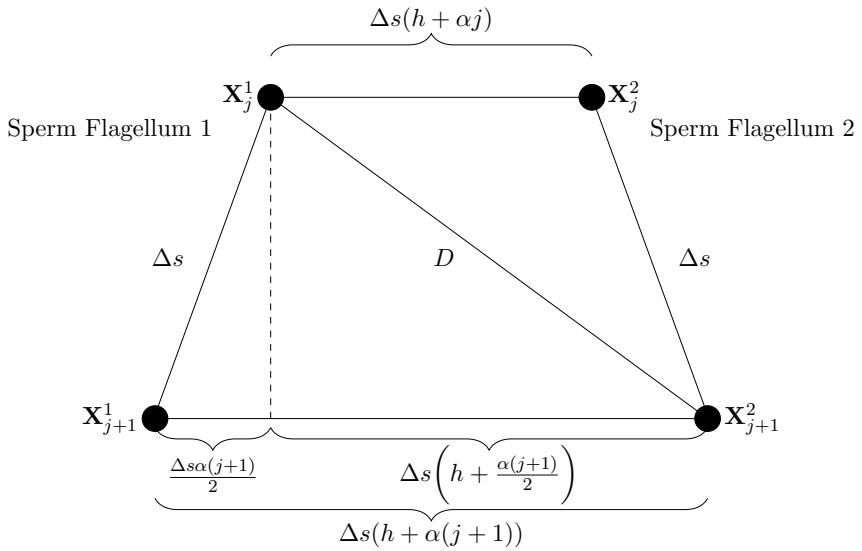

Figure 8: The trapezoidal geometry of two pairs of points on two connected flagella. D is the resting length of the diagonal spring force connecting points $\mathbf{X}_{j-1}^1$ and $\mathbf{X}_j^2$.

tions of sperm and more biologically-realistic modeling paradigms. These might include viscoelastic fluid models, in conjunction with biochemical signaling, changes in motility patterns over time, and—most importantly—the ability to find the egg and successfully fertilize it.

7 Conflict of interest statement

The authors have no conflicts of interest to disclose.

A Fused-head geometry

Figure 8 demonstrates the geometry involved in calculating the resting lengths for each spring connection in the fused-head model. In order to vary the angle between the first six points on the two flagella, we introduce the parameters h and α into our spring force calculation for the spring connecting points $\mathbf{X}_j^1$ and $\mathbf{X}_{j+1}^2$, labeled by length D in Figure 8. The parameter h specifies the resting length of the spring force between the first points on each flagellum, and α is used to incrementally increase the resting length of the spring force between each of the points as $j = 1, \ldots, 6$. Thus, α is used to fix the desired angle of fusion θ between the two flagella (see Figure 3c). A similar spring force will also be placed on the diagonal between $\mathbf{X}_j^2$ and $\mathbf{X}_{j+1}^1$ with the same resting length, for symmetry.

References

[1] MA Ball and GA Parker. Sperm competition games: inter-and intra-species results of a continuous external fertilization model. *Journal of Theoretical Biology*, 186(4):459–466, 1997.

[2] TR Birkhead, JG Martinez, T Burke, and DP Froman. Sperm mobility determines the outcome of sperm competition in the domestic fowl. *Proceedings of the Royal Society of London. Series B: Biological Sciences*, 266(1430):1759–1764, 1999.

[3] Ricardo Cortez. The method of regularized stokeslets. *SIAM Journal of Scientific Computing*, 23(4):1204–1225, 2001.

[4] Ricardo Cortez, Lisa Fauci, and Alexei Medovikov. The method of regularized stokeslets in three dimensions: analysis, validation, and application to helical swimming. *Physics of Fluids (1994-present)*, 17(3):031504, 2005.

[5] JM Cummins and PF Woodall. On mammalian sperm dimensions. *Journal of Reproduction and Fertility*, 75(1):153–175, 1985.

[6] Lisa J Fauci and Charles S Peskin. A computational model of aquatic animal locomotion. *Journal of Computational Physics*, 77(1):85–108, 1988.

[7] Heidi S Fisher and Hopi E Hoekstra. Competition drives cooperation among closely related sperm of deer mice. *Nature*, 463(7282):801–803, 2010.

[8] William D Hamilton. The genetical evolution of social behaviour. I. *Journal of Theoretical Biology*, 7(1):1–16, 1964.

[9] Fumio Hayashi. Insemination through an externally attached spermatophore: bundled sperm and postcopulatory mate guarding by male fishflies (megaloptera: Corydalidae). *Journal of Insect Physiology*, 42(9):859–866, 1996.

[10] Han-Chen Ho and Susan S Suarez. Hyperactivation of mammalian spermatozoa: function and regulation. *Reproduction*, 122(4):519–526, 2001.

[11] Simone Immler, Harry DM Moore, William G Breed, and Tim R Birkhead. By hook or by crook? Morphometry, competition and cooperation in rodent sperm. *PLoS One*, 2(1):e170, 2007.

[12] Steve D Johnston, Brett Smith, Michael Pyne, D Stenzel, and William V Holt. One-sided ejaculation of echidna sperm bundles. *The American Naturalist*, 170(6):E162–E164, 2007.

[13] I Llopis, I Pagonabarraga, M Cosentino Lagomarsino, and CP Lowe. Cooperative motion of intrinsic and actuated semiflexible swimmers. *Physical Review E*, 87(3):032720, 2013.

[14] JB Mackie and MH Walker. A study of the conjugate sperm of the dytiscid water beetles dytiscus marginalis and colymbetes fuscus. *Cell and Tissue Research*, 148(4):505–519, 1974.

[15] Michael Mesterton-Gibbons. On sperm competition games: raffles and roles revisited. *Journal of Mathematical Biology*, 39(2):91–108, 1999.

[16] Clément Mettot and Eric Lauga. Energetics of synchronized states in three-dimensional beating flagella. *Physical Review E*, 84(6):061905, 2011.

[17] Harry Moore, Katerina Dvorakova, Nicholas Jenkins, and William Breed. Exceptional sperm cooperation in the wood mouse. *Nature*, 418(6894):174–177, 2002.

[18] HD Moore. Gamete biology of the new world marsupial, the grey short-tailed opossum, monodelphis domestica. *Reproduction, Fertility and Development*, 8(4):605–615, 1996.

[19] HD Moore and DA Taggart. Sperm pairing in the opossum increases the efficiency of sperm movement in a viscous environment. *Biology of Reproduction*, 52(4):947–953, 1995.

[20] Tom Moore and Harry D Moore. Marsupial sperm pairing: a case of 'sticky' green beards? *Trends in Ecology & Evolution*, 17(3):112–113, 2002.

[21] Junko Ohmuro and Sumio Ishijima. Hyperactivation is the mode conversion from constant-curvature beating to constant-frequency beating under a constant rate of microtubule sliding. *Molecular Reproduction and Development*, 73(11):1412–1421, 2006.

[22] Sarah D Olson and Lisa J Fauci. Hydrodynamic interactions of sheets vs filaments: Synchronization, attraction, and alignment. *Physics of Fluids (1994-present)*, 27(12):121901, 2015.

[23] Sarah D Olson, Susan S Suarez, and Lisa J Fauci. Coupling biochemistry and hydrodynamics captures hyperactivated sperm motility in a simple flagellar model. *Journal of Theoretical Biology*, 283(1):203–216, 2011.

[24] Geoff A Parker and Tommaso Pizzari. Sperm competition and ejaculate economics. *Biological Reviews*, 85(4):897–934, 2010.

[25] Geoffrey A Parker. Sperm competition and its evolutionary consequences in the insects. *Biological Reviews*, 45(4):525–567, 1970.

[26] John J Parrish and Robert H Foote. Quantification of bovine sperm separation by a swim-up method relationship to sperm motility, integrity of acrosomes, sperm migration in polyacrylamide gel and fertility. *Journal of Andrology*, 8(4):259–266, 1987.

[27] Tommaso Pizzari and Kevin R Foster. Sperm sociality: cooperation, altruism, and spite. *PLoS Biology*, 6(5):e130, 2008.

[28] Julie Simons, Lisa Fauci, and Ricardo Cortez. Three-dimensional model of the interaction of driven elastic filaments in a stokes flow with applications to sperm motility. *Journal of Biomechanics*, 48:1639–1651, 2015.

[29] Julie Simons, Sarah Olson, Ricardo Cortez, and Lisa Fauci. The dynamics of sperm detachment from epithelium in a coupled fluid-biochemical model of hyperactivated motility. *Journal of Theoretical Biology*, 354:81–94, 2014.

[30] DJ Smith, EA Gaffney, H Gadêlha, N Kapur, and JC Kirkman-Brown. Bend propagation in the flagella of migrating human sperm, and its modulation by viscosity. *Cell Motility and the Cytoskeleton*, 66(4):220–236, 2009.

[31] SS Suarez and Xiaobing Dai. Hyperactivation enhances mouse sperm capacity for penetrating viscoelastic media. *Biology of Reproduction*, 46(4):686–691, 1992.

[32] Geoffrey Taylor. Analysis of the swimming of microscopic organisms. In *Proceedings of the Royal Society of London A: Mathematical, Physical and Engineering Sciences*, volume 209, pages 447–461. The Royal Society, 1951.

[33] Geoffrey Taylor. The action of waving cylindrical tails in propelling microscopic organisms. *Proceedings of the Royal Society of London. Series A, Mathematical and Physical Sciences*, pages 225–239, 1952.

[34] John L VandeBerg and Sarah Williams-Blangero. The laboratory opossum. In *The UFAW Handbook on the Care and Management of Laboratory and Other Research Animals*, pages 246–261. Wiley-Blackwell, West Sussex, UK, 2010.

[35] G Vernon and D Woolley. Basal sliding and the mechanics of oscillation in a mammalian sperm flagellum. *Biophys. J.*, 85(6):3934–3944, 2004.

[36] David M Woolley, Rachel F Crockett, William DI Groom, and Stuart G Revell. A study of synchronisation between the flagella of bull spermatozoa, with related observations. *Journal of Experimental Biology*, 212(14):2215–2223, 2009.

[37] Yingzi Yang, Jens Elgeti, and Gerhard Gompper. Cooperation of sperm in two dimensions: synchronization, attraction, and aggregation through hydrodynamic interactions. *Physical Review E*, 78(6):061903, 2008.